

2-DOF Synchronous Electrostatic Actuator with Transparent Electrodes Arranged in Checkerboard Patterns

Takuya Hosobata¹, Akio Yamamoto¹, and Toshiro Higuchi¹

Abstract—This paper reports a 2-DOF electrostatic actuator with all electrodes made with transparent materials. The actuator is composed of two plastic films, a stator film and a slider film. The two films are sectioned into four-by-four checkerboard patterns, whose squares include fine-pitched strip electrodes arranged in orthogonal directions. A pair of three-phase voltages drives the slider in open-loop, along any preset paths in the 2-D plane. A prototype was fabricated with etched indium tin oxides and screenprinted conductive polymers. With 500 V excitation, the prototype exerted 60 to 100 mN forces in eight directions, and the slider traveled along straight and circular paths within its operating range of 132 mm by 132 mm, at maximum speed of 240 mm/s. With the transparency, the actuator realizes collaboration of an actuated physical object and animated images, on surfaces of flat panel displays.

I. INTRODUCTION

Electrostatic actuators can be made transparent, because the only two components they require are conductors and insulators, both of which are available in transparent materials. Based on this idea suggested by Egawa et al. [1], we report in this paper a 2-DOF transparent electrostatic actuator, which enables actuation of physical objects on top of Flat Panel Displays (FPDs).

In 1997, Ullmer and Ishii proposed that human computer interaction is enriched with a coexistence of real “tangible” objects with digital information [2]. One implementation of the idea is a tabletop interface, in which the tangible objects and displayed images can collaborate on a single surface [3]. Such interface is further improved when the objects are actuated. For this purpose, use of planar magnetic actuators have been proposed, which include an array of electromagnets [4], a Sawyer motor [5] and a linear induction motor [6].

Magnetic actuators are suited for tabletop interfaces with projectors, because they require spaces beneath the tabletop surface for their stators. However, they are difficult to integrate with FPDs and rear-projection displays, which are favorable over projectors for not projecting images to the objects placed on top.

One solution to realize a tabletop interface without using a projector is to use extracted panel of an FPD with magnetic actuators, through which magnetic flux can penetrate [7]. A drawback of this solution is that it requires modifications on the FPD. Another solution is to use wheeled robots as in

[8] and [9], to append the objects themselves the actuation capabilities. However, the sizes of the robots may become a problem in some applications; robots are difficult to down-size, because they carry batteries and driver electronics.

As a simpler way to realize an actuation on a display surface, Amano and Yamamoto from our research group have recently proposed the use of transparent electrostatic actuators [10]. The actuator is transparent because it is made of a PolyEthylene Terephthalate (PET) film with Indium Tin Oxide (ITO) electrodes, and it can actuate paper sheets with a three-phase voltage applied to the electrodes. Thus, simply placing this actuator on top realizes an actuation on an FPD surface. However, because the actuator had only 1-DOF, the motion it could realize was limited to simple back-and-forths. Therefore, development of a transparent actuator with 2-DOF became our next goal.

In this paper, we introduce a transparent 2-DOF electrostatic actuator. We designed the actuator based on a dual excitation type electrostatic film actuator [11], which operates in a different principle from the previous paper sheet actuator. The dual excitation actuator is a synchronous actuator, whereas the paper sheet actuator is an asynchronous actuator. We chose the synchronous actuator because it is easier to control; we are able to control the slider’s position in open-loop.

The 2-DOF electrostatic actuator is composed of two transparent films: a stator film and a slider film. The stator film has fine-pitched three-phase electrodes patterned with an etched ITO. The stator is sectioned into checkerboard squares, in which electrodes for driving in two directions are separated. Peripheral lines connecting the electrodes to the voltage sources are also transparent, screenprinted with conductive polymers. The slider film is a smaller sized checkerboard, with all patterns screenprinted with conductive polymers. Applying three-phase voltages to the electrodes drives the slider along any path within the stator surface. Thus, with the actuator placed on an FPD, we can easily synchronize the motion of the slider with animated images.

Remainder of this paper is as follows. Section II describes the design concept of the actuator. The novelty of the actuator is in its checkerboard-patterned structure, and the key factor in design is the relative sizes and numbers of squares in the two checkerboards. In Section III, the fabrication process of the transparent films is explained. Then, experimental results regarding the thrust force and 2-DOF planar motion is given in Section IV, and a conclusion follows in Section V.

This work was supported by Funding Program for Next Generation World-Leading Researchers (#LR013) from JSPS, Japan.

¹The authors are with the Department of Precision Engineering, School of Engineering, the University of Tokyo, 7-3-1 Hongo, Bunkyo-ku, Tokyo, Japan. {hosobata, akio, higuchi} at aml.t.u-tokyo.ac.jp.

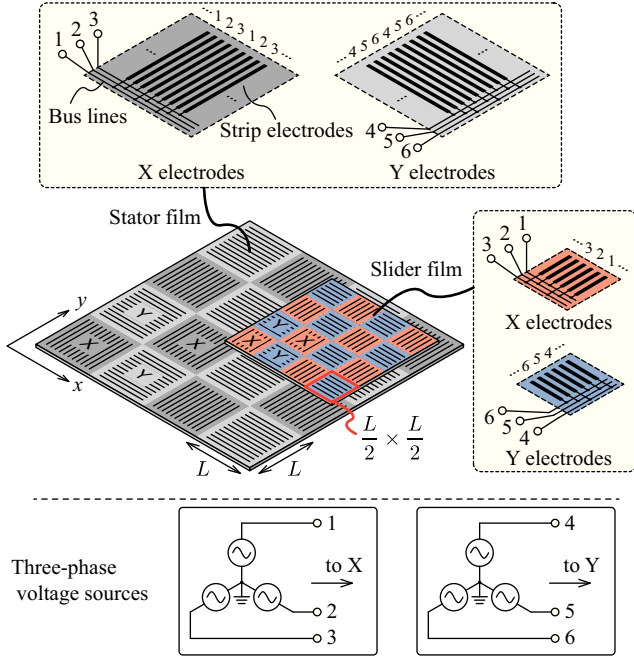


Fig. 1. Schematic of 2-DOF planar electrostatic actuator.

II. DESIGN CONCEPT

A. Structure of 2-DOF Electrostatic Actuator

Fig. 1 shows a schematic of the 2-DOF planar electrostatic actuator. The actuator consists of two films: a stator film and a slider film, both sectioned into four-by-four checkerboard patterns. The only difference between the stator and the slider is the size of squares; sides of slider squares are half that of the stator squares.

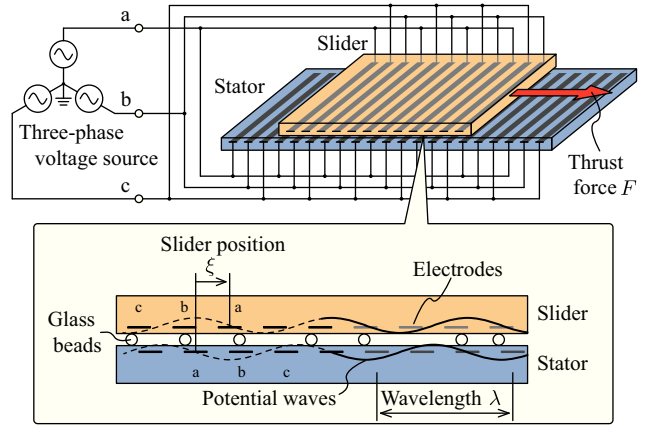
Each square of the checkerboard has fine-pitched strip electrodes, connected in a three-phase pattern. Electrodes in each square are arranged in directions perpendicular to those in the neighboring squares. For clarity, we refer to the electrodes of different directions as the X and Y electrodes.

A pair of three-phase voltage sources drives the actuator. Numbers one to six in the figure indicate the correspondence of electrodes and the sources. Note that the electrodes in the stator and the slider are connected to the sources in an opposite phase sequence. Excited by the voltage sources, the X electrodes of the stator and the slider interact with each other to produce thrust force in the x direction, and the same applies to the Y electrodes. Thus, controlling the pair of three-phase voltages realizes a 2-DOF planar actuation.

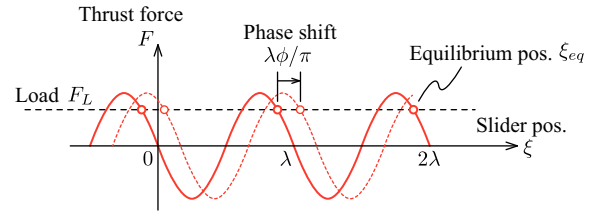
The operating principle of the actuator is explained in following sections. First, a brief explanation is given on an 1-DOF actuator. Then, we explain how the units of this actuator are integrated into checkerboard patterns to realize seamless 2-DOF actuation.

B. Characteristic of 1-DOF Electrostatic Actuator

An 1-DOF electrostatic film actuator is illustrated in Fig. 2a. The actuator consists of a slider film and a stator film with three-phase electrodes embedded in their insulating



(a) Schematic of electrostatic film actuator (1-DOF).



(b) Ideal force characteristic.

Fig. 2. Schematic of 1-DOF electrostatic actuator and ideal position-force curve.

substrates. The two films are facing across a short gap, which is maintained by glass beads.

To the electrodes, a three-phase voltage is applied in opposite phase sequences. The applied voltages form potential waves on the films. The waves have a fundamental wavelength of λ , which is equal to three times the electrode pitch. When the two potential waves are spatially displaced from each other, the electric field in the gap gives thrust to the slider. If we define the three-phase voltage with an amplitude V and a temporal phase ϕ as

$$[v_a \ v_b \ v_c] = V [\sin \phi \ \sin (\phi - 2\pi/3) \ \sin (\phi + 2\pi/3)], \quad (1)$$

an ideal thrust force F of the actuator is expressed as

$$F = -KV^2 \sin (2\pi\xi/\lambda - 2\phi), \quad (2)$$

where K is a constant in units of N/V^2 and ξ is the slider's position. The thrust force is expressed as a function of the position ξ and the phase ϕ because both of these are relevant to the spatial displacement of the potential waves.

The force characteristic enables us to control the slider position in open-loop. Fig. 2b is an ideal position-force curve. When a constant load $F_L \leq KV^2$ is working against the thrust force, the equilibrium position ξ_{eq} : the position where the slider balances in steady-state is

$$\xi_{eq} = \frac{\lambda}{2\pi} \left(2\phi - \sin^{-1} \frac{F_L}{KV^2} \right). \quad (3)$$

The expression is multi-valued, indicating that there are multiple equilibrium positions. The equilibrium positions are

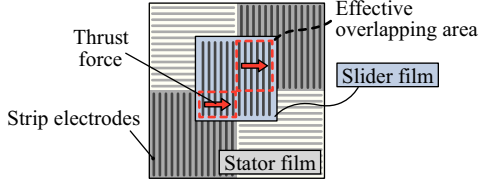


Fig. 3. Definition of effective overlapping area of electrodes.

shifted by changing the value of ϕ . Thus, the slider travels together with the equilibrium position at which it is initially balanced.

Another important characteristic to note is that the actuator is passively stable in yaw rotation; within a tolerable angular displacement, there is a moment acting on the slider electrodes to restore their parallelism with the stator electrodes. Analysis of the yaw stability is given in [12]. The yaw stability is also inherited to the 2-DOF actuator.

C. Integration of 1-DOF Units into Checkerboard Patterns

To construct a 2-DOF actuator from the units of 1-DOF actuators, the X and Y electrodes must coexist within a same plane. First, for the stator, we chose to arrange the X and Y electrodes in a checkerboard pattern. The problem was to find out the arrangement of electrodes for the slider.

An important concept to consider was the change of effective overlapping area with the slider's position. The effective overlapping area is defined as the area with the electrodes of the same direction overlapped, as illustrated in Fig 3. The term effective indicates that only the parts of electrodes within this area contribute in producing thrust force. This is because a pair of potential waves spatially periodic in the same directions produces the thrust force.

The effective overlapping area may vary with slider position, thus the area must be included in the thrust force equations. Assuming that a pair of three-phase voltages with amplitude of V and temporal phases of ϕ_x and ϕ_y ,

$$\begin{cases} v_1 = V \sin \phi_x \\ v_2 = V \sin (\phi_x - 2\pi/3) \\ v_3 = V \sin (\phi_x + 2\pi/3) \end{cases}, \begin{cases} v_4 = V \sin \phi_y \\ v_5 = V \sin (\phi_y - 2\pi/3) \\ v_6 = V \sin (\phi_y + 2\pi/3) \end{cases} \quad (4)$$

are applied to the electrodes, we can extend (2) for a 2-DOF actuator as

$$\begin{cases} F_x = -kA_x(x, y) V^2 \sin (2\pi x/\lambda - 2\phi_x) \\ F_y = -kA_y(x, y) V^2 \sin (2\pi y/\lambda - 2\phi_y) \end{cases} \quad (5)$$

The constant k is in units of $\text{N}/\text{V}^2/\text{m}^2$, A is the effective overlapping area, and subscripts x and y in all symbols indicate that the symbols are related to the specified direction. To realize a 2-DOF actuator capable of continuous operation in the whole area of the stator, the slider must be designed such that the overlapping areas A_x and A_y become independent of positions x and y .

We found that designing the slider film in a half-sized checkerboard pattern realizes the consistency of effective

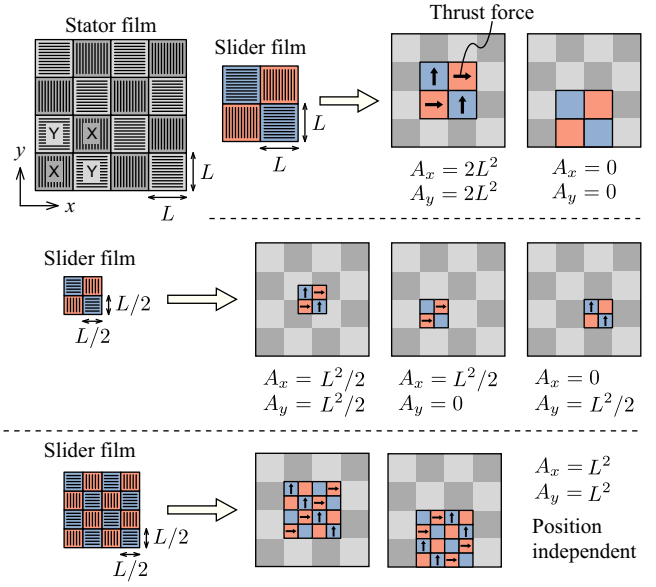


Fig. 4. Checkerboard patterns with different sizes and numbers of squares in slider. Inadequate design causes position dependence in effective overlapping areas A_x and A_y .

overlapping areas. Fig. 4 shows such design, together with two examples of inadequate designs. In the inadequate examples, one or both of the X/Y electrodes become completely separated from their counterparts at specific slider positions; consequently, the thrust force is lost at these conditions. On the other hand, with the four-by-four half-size design, half of the X/Y electrodes in the slider are always overlapping with their counterparts in the stator, regardless of the slider position. Thus, the effective overlapping areas become position independent, always one fourth of the slider's total area.

With the assumption that overlapping areas A_x and A_y are constant, the equilibrium position of the slider under a load with force components $F_{Lx} \leq kA_x V^2$ and $F_{Ly} \leq kA_y V^2$ is given as

$$\begin{cases} x_{eq} = \frac{\lambda}{2\pi} \left(2\phi_x - \sin^{-1} \frac{F_{Lx}}{kA_x V^2} \right) \\ y_{eq} = \frac{\lambda}{2\pi} \left(2\phi_y - \sin^{-1} \frac{F_{Ly}}{kA_y V^2} \right) \end{cases} \quad (6)$$

Thus, a smooth 2-DOF in-plane motion is realized in open-loop, by shifting the temporal phases ϕ_x and ϕ_y to have the equilibrium position tracing a desired path.

It should be noted that the position independence does not perfectly apply to the actual films. As explained in the next section, the checkerboard squares are not fully occupied with fine-pitched electrodes; there are areas with bus lines, which are ineffective in terms of producing thrust force. However, the position dependence was sufficiently small for the prototype motor to realize a smooth 2-DOF motion.

III. FABRICATION OF FILMS

This section describes the fabrication process of the stator film and slider film. The most important factor in

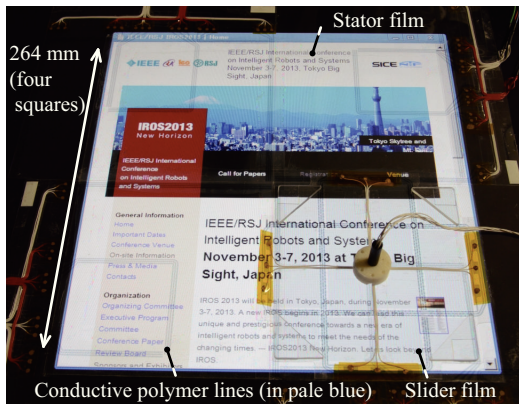


Fig. 5. Photograph of 2-DOF transparent electrostatic actuator on FPD.

design was to make the electrodes appear as transparent as possible. Thus, as the material for the stator electrodes covering the FPD surface, we chose to use ITO. For the materials for the rest of the patterns, we chose a conductive polymer poly(3,4-ethylenedioxythiophene):poly(4-styrenesulfonate) (PEDOT:PSS), which is available as inks for screenprinting. Fig. 5 is the photograph of the fabricated films placed on top of an FPD. The ITO electrodes are invisible, whereas the lines printed with the polymer are translucent, visible in pale blue. However, especially with the help of FPD backlight, the polymers are transparent enough for us to see through them to the displayed images.

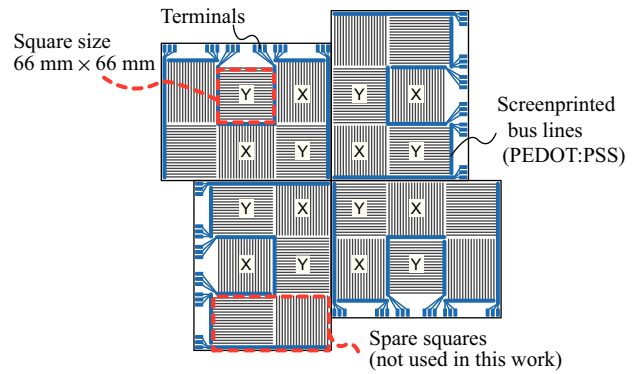
A. Stator Film

Fig. 6a shows the design of the stator film. In this particular work, we separated the stator into four films, due to practical limitation by the substrate size. However, the separation is not essentially important, because the following process applies to the cases using larger substrates, just as well. Appearance of a single film is shown in Fig. 6b. Each film contains six squares with their length of sides 66 mm; two out of which are spares, not used in this work.

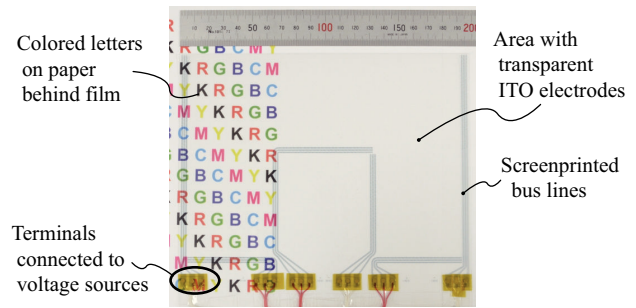
Fig. 6c shows the procedure of fabrication. A PET film with ITO sputtered on its surface was prepared, and the ITO was etched into strip electrodes with a pitch of 400 μm . To connect these electrodes in a three-phase pattern, vias were made by screenprinting. First, an interlayer insulator with holes was formed on top of the ITO electrodes, using a thermosetting insulating paste (FR-1T-NSD9, Asahi Chemical Research Laboratory). Then, using an ink of PEDOT:PSS (Orgacon EL-P5015, Agfa-Gavert Group), bus lines were printed on top of this insulating layer, which became connected with the ITO electrodes through the holes. Finally, whole surface of the film was covered with another insulating layer and a protection film.

B. Slider Film

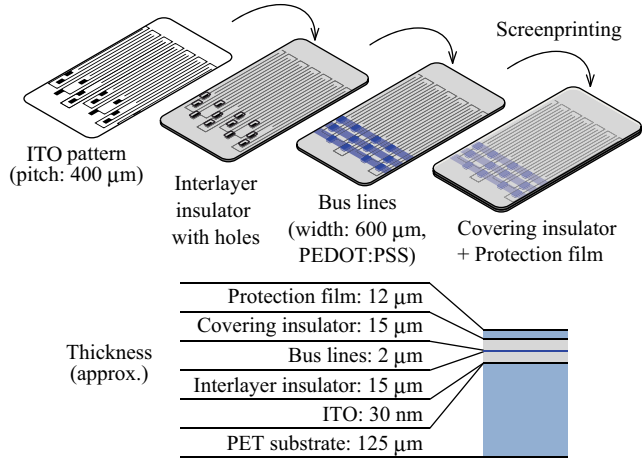
Slider film has a structure similar to the stator, except for the following. First, all patterns of conductors are screenprinted on a blank sheet of PET with a PEDOT:PSS ink. Second, the length of the sides of squares is 33 mm: half



(a) Stator with four films arranged in rotational symmetry.



(b) Photograph of a stator film.



(c) Pattern details.

Fig. 6. Design of the stator film. Photograph (b) is taken on top of a paper with colored letters to demonstrate transparency. PET film used for surface protection is Kimotect PA-12X(Kimoto Co.).

that of the stator. Other parameters are the same with the stator, including electrode pitch, insulating materials and their thickness.

Fig. 7 is the photograph of the slider, and notable features are as follows. First, flexible wires (NEF-34-1646 Cooner Wire) are used to minimize the disturbance to the slider's motion. We fixed the wires at the center of the slider to avoid yaw moments caused by the pulling of the wires. Second, acrylic plates are placed at the corners of the film, acting as weights. The weights assure the slider film to be pressed against the stator, to maintain the gap between the films; the

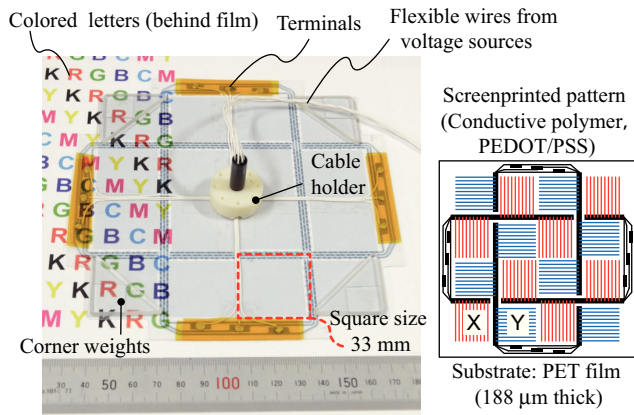


Fig. 7. Structure of the slider made by screenprinting. The slider weighs 20 grams including cable holder and corner weights.

slider film was slightly curled due to the printing of insulator. Including weights, the slider weighed 20 g.

IV. EXPERIMENTAL RESULTS

We conducted two experiments to check the basic performance of the actuator. The first experiment is a force measurement in eight directions. Second is an open-loop driving of the slider along straight and circular paths. In all experiments, voltage amplitudes were set to 500 V, below the breakdown voltage of the insulator, which was around 600 V. Glass beads with 100 μm diameter were scattered between the films for gap maintenance and lubrication.

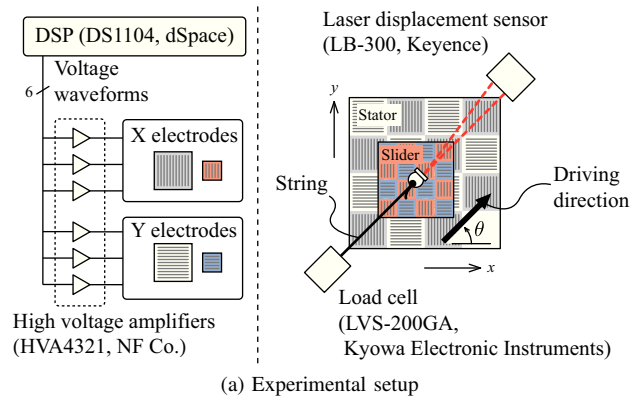
A. Force Measurement

Force measurements were conducted using the setup shown in Fig. 8a. The slider was driven in the direction θ , at a speed of $u = 10$ mm/s, while being pulled by an elastic string. To realize such motion, the phases ϕ_x and ϕ_y of the voltages in (4) were respectively set to $\phi_x = (\pi u \cos \theta / \lambda) t$ and $\phi_y = (\pi u \sin \theta / \lambda) t$. Tension of the string was measured using a load cell, and an example of the measured data is shown in Fig. 8b. The slider stepped out when the tension reached a certain value, which is equal to the actuator's maximum force. A ripple observed during the travel had spatial period equivalent to the electrode pitch.

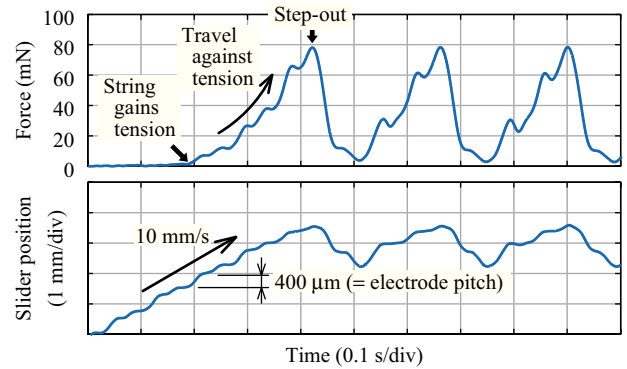
Fig. 8c shows the maximum force of the actuator in eight different directions. The results show that the maximum forces in orthogonal directions is approximately 60 mN, and that in diagonal directions is around 95 mN. The force is larger in diagonal directions, because the force is a vector sum of the forces produced by X and Y electrodes. Variations in the measured forces come from three factors that could not be controlled precisely: friction (amount of glass beads), local step-out position, and disturbance from feeding wires.

B. 2DOF Motion

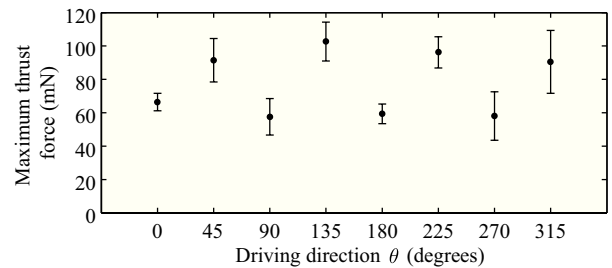
The slider is able to travel along any path within the square of 132 mm \times 132 mm, with the load applied to the slider not exceeding the maximum force. The load includes an inertial force, a friction between the films and a tension from



(a) Experimental setup



(b) Example of measured data ($\theta = 0^\circ$)



(c) Driving direction vs. maximum thrust force.

Fig. 8. Method and results of force measurement. Voltage amplitude was set to 500 V, and the forces were measured 10 times for each direction.

feeding wires. In designing motion paths, the acceleration of the motion was limited to 0.25 m/s^2 , which is an empirical maximum acceleration for stable motion. The wires were carefully put on the stator surface so as not to disturb the slider motion.

Fig. 9 shows the result of motion tracking while the slider traveled three straight paths in x , y and diagonal directions in sequence. For motion tracking, we used high-speed camera (VW-6000, Keyence). The capturing speed and spatial resolution was set to 250 frames per second and 480 $\mu\text{m}/\text{pixel}$, respectively. Dynamic range of the measurement was insufficient to evaluate the position error from the reference trajectory; however, we can say that the error was within the length of three electrode pitches (1.2 mm) because the slider did not step out during the motion. The slider could reach the top speed of 170 mm/s in orthogonal directions,

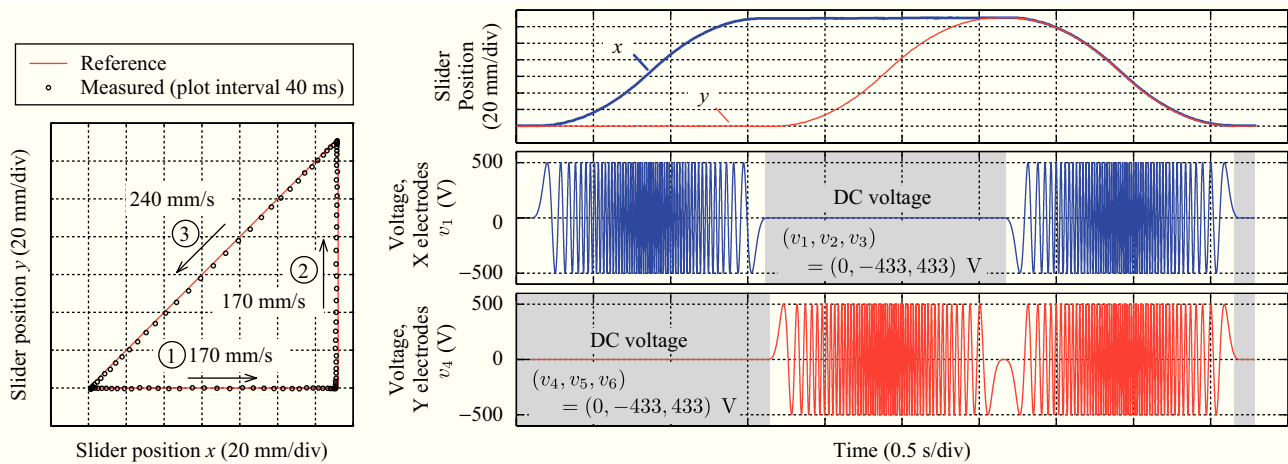


Fig. 9. Sequential linear motion of the slider and patterns of applied voltages.

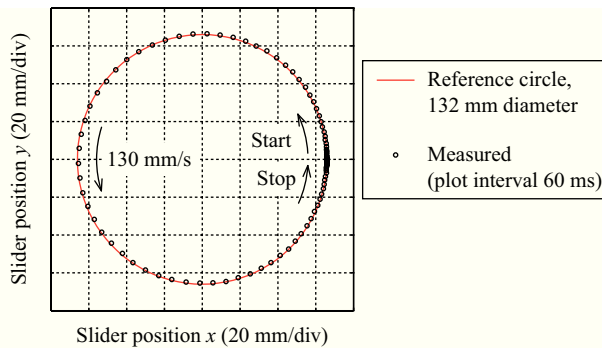


Fig. 10. Circular motion of the slider.

and 240 mm/s in a diagonal direction. The voltage patterns applied to the X and Y electrodes are also shown in the figure. When the slider is traveling in x direction, three-phase AC voltage with variable frequency is applied to the X electrodes, and a set of DC voltages are applied to the Y electrodes. In this case, the Y electrodes are serving as a linear guide. During the diagonal motion, both of the X and Y electrodes are excited with the three-phase AC voltages. The slider could also travel along curved paths. As an example, a circular motion of 132 mm diameter is shown in Fig. 10. This circular trajectory was set so that the resultant of centripetal and tangential accelerations stays within the limit. The maximum tangential speed realized was 130 mm/s.

V. CONCLUSION

In this paper, a transparent 2-DOF electrostatic actuator was proposed. A working prototype was developed, which demonstrated its capabilities to exert forces in different directions and to travel along 2-D paths. With the transparency, the actuator allows an actuated object to coexist with displayed images on an FPD. Through this work, we found some challenges to overcome. First, the thrust force needs to be increased, because the prototype could tolerate only small disturbances and no tilting of the driving surface. Second,

an actuator with multiple sliders needs to be developed, to broaden the scope of application. Finally, we must find a way to realize the synchronous driving without the electrical wires to the slider, because the wires appear obtrusive on FPDs, and will cause problems with multiple sliders as the wires may become entangled. We hope to push the development further towards practical application of the actuator.

REFERENCES

- [1] S. Egawa, T. Niino and T. Higuchi, Film actuators: Planar, electrostatic surface-drive actuators, In Proc. of the IEEE Micro Electro Mechanical Systems Workshop, 1991, pp. 9–14.
- [2] H. Ishii and B. Ullmer, Tangible bits: towards seamless interfaces between people, bits and atoms. In Proc. of the SIGCHI Conf. on Human Factors in Computing Systems, 1997, pp. 234–241.
- [3] B. Ullmer and H. Ishii, The metaDESK: models and prototypes for tangible user interfaces. In Proc. of the 10th Annual ACM Symposium on User Interface Software and Technology, 1997, pp. 223–232.
- [4] G. Pangaro, D. Maynes-Aminzade and H. Ishii, The actuated workbench: computer-controlled actuation in tabletop tangible interfaces. In Proc. of the 15th Annual ACM Symposium on User Interface Software and Technology, 2002, pp. 181–190.
- [5] M. Sugi et al., Motion Control of Self-Moving Trays for Human Supporting Production Cell “Attentive Workbench”, In Proc. of the IEEE International Conf. on Robotics and Automation, 2005, pp. 4080–4085.
- [6] S. Yoshida, H. Noma, and K. Hosaka, Proactive Desk II: Development of a New Multi-object Haptic Display Using a Linear Induction Motor, In IEEE Virtual Reality Conf., 2006, pp.269–272.
- [7] M. Weiss et al., Madgets: actuating widgets on interactive tabletops, In Proc. of the 23rd Annual ACM Symposium on User Interface Software and Technology, 2010, pp. 293–302.
- [8] E. W. Pedersen and K. Hornbæk, Tangible bots: interaction with active tangibles in tabletop interfaces, In Proc. of the 2011 Annual Conf. on Human Factors in Computing Systems, 2011, pp. 2975–2984.
- [9] H. Mi, A. Krzywinski, T. Fujita and M. Sugimoto, RoboTable: An Infrastructure for Intuitive Interaction with Mobile Robots in a Mixed-Reality Environment, Advances in Human-Computer Interaction, 2012, Article ID 301608, 10 pages
- [10] K. Amano and A. Yamamoto, Tangible interactions on a flat panel display using actuated paper sheets, In Proc. of the ACM Int. Conf. on Interactive Tabletops and Surfaces, 2012, pp. 351–354.
- [11] T. Niino, T. Higuchi and S. Egawa, Dual excitation multiphase electrostatic drive, In: Proc. of the IEEE Industry Applications Society Annual Meeting, 1995, vol. 2, pp. 1318–1325.
- [12] A. Yamamoto et al., Performance improvement of electrostatic actuator by skewing electrodes, In: Proc. of the IEEE Industry Applications Society Annual Meeting, 1996, vol. 4, pp. 1980–1985.